Calculation and correction of piston phase aberration in synthesis imaging

Richard J. Eastwood,[1,2,*] Anne Marie Johnson,[1,3] and Alan H. Greenaway[1]

[1]*Physics, Scottish Universities Physics Alliance/Institute of Integrated Systems, School of Engineering and Physical Sciences, Heriot-Watt University, Edinburgh, EH14 4AS, Scotland*
[2]*Current address: Department of Physics, The University of Hull, Hull HU6 7RX, UK*
[3]*Current address: Spacecraft Research and Design Center, Department of Mechanical and Astronautical Engineering, Naval Postgraduate School, Monterey, California 93943, USA*
**Corresponding author: r.j.eastwood@physics.hull.ac.uk*

Received March 3, 2008; revised October 17, 2008; accepted October 17, 2008; posted November 19, 2008 (Doc. ID 93266); published December 24, 2008

The principle of redundant spacings calibration has previously been described for the purpose of calibrating piston phase aberration affecting elements of a dilute aperture array using a system of linear equations in terms of the aperture phases as well as object phase information. Here we develop matrices for the correction of piston phase aberration by use of image sharpness and also by phase retrieval. These are both presented in wavefront sensor formulation in order to draw analogy between the approaches. We then discuss solution ambiguity affecting both methods and describe array design criteria to prevent such ambiguity. The problem of increased image aliasing under image sharpness correction is also highlighted. © 2008 Optical Society of America

OCIS codes: 110.5100, 110.1220, 110.5050, 110.1080.

1. INTRODUCTION

"Seeing," as produced by layers of turbulent "atmosphere," leads to image distortion at frequencies from radio to the visible as the point-spread function (PSF) of the imaging system loses sharpness and symmetry. At shorter wavelengths the development of conventional adaptive optics (AO) for filled apertures using, for example, Shack–Hartmann wavefront sensors and deformable mirrors, has demonstrated considerable success, ameliorating much of the atmospheric distortion and thereby restoring performance closer to the diffraction limit [1]. Synthetic imaging systems, such as are well known in astronomical radio interferometry, offer greater maximum aperture dimension than is possible with a single collector, giving a commensurate increase in resolution. For this reason they are becoming more widespread in optical observation [2–4] and also recently in military surveillance applications [5], where single large apertures are not practicable.

In synthesis imaging each collector in the dilute aperture is "seeing" through a different aberrating patch, though each patch may be correlated with its neighbors. The resulting PSF is an Airy-disk-shaped envelope function modulating interference fringes whose period and orientations depend on the array design. Phase errors distort the interferogram and subsequent object reconstruction.

In radio astronomy the collectors can acceptably be treated as δ functions sampling the wavefront, so that the phase aberration over any collector is considered piston only. When making the transition to the optical domain, not only does the phase of incoming wavefronts have to be measured indirectly (using quadrature rather than heterodyne detection) but also the phase profile will not be limited to just a piston component. However for moderate atmospheric conditions with correlation patch size of the order of the aperture size, piston phase is a reasonable approximation to the aberration.

The focus of this paper is the phase calibration of optical wavefronts by redundant spacings calibration (RSC) [6]. As will be described below, RSC is a method that permits the separation of instrument-dependent and object-dependent phase information for extended sources. By this means the object brightness distribution can be uniquely estimated without the use of any object-specific assumptions.

It is assumed here that the imaging conditions are isoplanatic, that the instrument consists of many apertures of the same size and shape, and that redundancies in the instrument layout correspond to identical vector spacing between the apertures in the array. The first of these assumptions is common in high-resolution astronomy, the second easily achieved with appropriate accuracy in macroscopic optical systems, and the last found by experience to be reasonable, provided that vector spacings are equal to an accuracy of $\sim$10% of the diameter of the individual apertures. This paper will treat only piston errors of apertures subject to uniform illumination; generalization to higher-order and nonuniform illumination will be presented in following papers.

In previous formulation, RSC required Fourier transformation of the interferogram/image followed by (explicitly or implicitly) taking a logarithm of the complex data to extract phases that can be used with matrix algebra to calibrate the instrument and to extract object Fourier phases. This procedure had the disadvantages that it gave equal weight to all object Fourier components irre-

spective of the associated fringe visibility, and it introduced modulo arithmetic that can result in a finite (generally small) set of ambiguous solutions even when the matrix equations are full rank.

Here we show that analysis based in "image sharpness" can be used on the same data to apparently circumvent the Fourier weighting problem. Use of image sharpness reveals new subtleties in array design criteria and this, along with analysis in terms of matrix algebra, has allowed us to identify methods for avoiding ambiguity that do not compromise the imaging properties of the array and are equally applicable to the phase extraction method and image sharpness.

Previous papers have described RSC in terms of piston phase correction. Although solution by inversion has been discussed [6], it is presented in Section 2 in a different form for comparison with an approach for correction of phases by the maximization of image sharpness. We derive, from the presence of some identical repeated spacings in a dilute aperture, systems of equations in aperture phases that describe the image sharpness calibration and are also applicable to the phase retrieval approach, solvable by data inversion. These methods allow unique calibration of instrumental piston error. The fidelity of images reconstructed from incomplete frequency sampling of object information is also considered. Section 3 examines the potential introduction of ambiguity due to the arithmetic being modulo 2π in nature and describes array design methods to avoid this. Section 4 is a discussion of the results in terms of their usefulness and limitations.

2. REDUNDANT SPACINGS CALIBRATION

We begin by deriving the fundamental relationships on which synthesis imaging is based, before restricting consideration to the case of piston-only aberrations of apertures subject to uniform illumination. Solution methods for RSC are then investigated and the effect of any violation of assumptions treated qualitatively.

A. Fundamental Relationships

From the van Cittert–Zernike theorem [7], imaging an incoherent scene with brightness function u through turbulent atmosphere and ignoring anisoplanatism so that the wavefront arriving at the aperture array from each point on the source is described by function $\mathcal{L}$ yields an image with irradiance distribution

$$I(\xi) = \int R_{\mathcal{L}}(\alpha) U(\alpha) \exp(-i\xi \cdot \alpha) \mathrm{d}\alpha = \mathcal{F}[R_{\mathcal{L}} U], \qquad (1)$$

with the optical transfer function (OTF) $R_{\mathcal{L}}$ being the autocorrelation of the complex wavefront function in the form

$$R_{\mathcal{L}}(\alpha) = \int \mathcal{L}^*(r) \mathcal{L}(r-\alpha) \mathrm{d}r. \qquad (2)$$

U is the two-dimesional Fourier transform of the brightness distribution and ξ the imaging spatial frequency vector. Thus, the information in the object's Fourier transform is modulated by the OTF.

Supposing wavefront function $\mathcal{L}(r) = m(r)\exp[i\tilde{\varphi}(r)]$ is sampled by an aperture function A consisting of individual circular apertures a of identical diameter distributed across it, the sampled wavefront function will be $L = \mathcal{L}A$. Writing the aperture function A as the convolution of the circular function with a set of shifted δ functions representing the aperture locations yields

$$A(r) = \sum_{j \in \mathcal{A}} a(r - r_j); \qquad \begin{cases} a(s) = 1 & |s| \leqslant \rho \\ = 0 & |s| > \rho \end{cases}, \qquad (3)$$

where $\mathcal{A}$ denotes the set of apertures, r_j is the vector location of each, and ρ is their (identical) radius. L is then given by

$$L(r) = \mathcal{L}(r) \sum_{j \in \mathcal{A}} a(r - r_j) = \sum_{j \in \mathcal{A}} m_j(r - r_j) \exp[i\tilde{\varphi}_j(r - r_j)], \qquad (4)$$

with m_j and $\tilde{\varphi}_j$ the illumination and phase functions, respectively, of the wavefront over each aperture j. The autocorrelation from Eq. (2) thus becomes

$$\begin{aligned} R_L(\alpha) &= \int L^*(r) L(r-\alpha) \mathrm{d}r \\ &= \sum_{j \in \mathcal{A}} \sum_{k \in \mathcal{A}} \int m_j(r - r_j) \exp[-i\tilde{\varphi}_j(r - r_j)] m_k(r - r_k - \alpha) \\ &\quad \times \exp[i\tilde{\varphi}_k(r - r_k - \alpha)] \mathrm{d}r, \end{aligned} \qquad (5)$$

thereby expressing the imaging process of Eq. (1) in terms of the wavefront aperture phase functions $\tilde{\varphi}_j$. We therefore make use of the information in R_L for studying methods of phase correction and calculation; this is particularly useful for understanding and taking advantage of simplifying assumptions about the imaging system and conditions.

B. Piston Phases Only

Restricting the preceding discussion such that the wavefront phase at each aperture is piston only, i.e., a constant function, the autocorrelation is correspondingly

$$R_L(\alpha) = \sum_{j \in \mathcal{A}} \sum_{k \in \mathcal{A}} \exp[i(\tilde{\varphi}_k - \tilde{\varphi}_j)] \int m_j(r - r_j) m_k(r - r_k - \alpha) \mathrm{d}r. \qquad (6)$$

To simplify the mathematics we now discuss the explicit representation of R_L as the combination of cross correlations of aperture pairs in L,

$$R_L(\alpha) = \sum_{j \in \mathcal{A}} \sum_{k \in \mathcal{A}} R_{jk}(\alpha - s_{jk}), \qquad (7)$$

with s_{jk} the spacing between the jth and kth apertures and R_{jk} the cross correlation given by

$$\begin{aligned} R_{jk}(\alpha') &= \exp[i(\tilde{\varphi}_k - \tilde{\varphi}_j)] \int m_j(r') m_k(r' - \alpha') \mathrm{d}r' \\ &= M_{jk}(\alpha') \exp[i(\tilde{\varphi}_k - \tilde{\varphi}_j)], \end{aligned} \qquad (8)$$

where $M_{jk}(\alpha')$ is the magnitude only cross correlation of two diffraction-limited apertures. For the remainder of

this work we will assume uniform illumination so that m_j is unity within the aperture radius. Thus, as shown by the shaded area in Fig. 1, $M_{jk}(\alpha')=\int_{r\in C(\alpha')}dr$, where $C(\alpha')$ is the area of overlap at relative shift α', forming peaks in the magnitude component of R_L and piston-only patches with values given by $\tilde{\varphi}_k-\tilde{\varphi}_j$ in the phase part.

C. Correcting Piston Aberration by Image Sharpness RSC

Under the above assumptions it can be seen from Eq. (1) that a sufficient condition for the image I to be free of distortion is that the phase of the sampled wavefront autocorrelation $\angle R_L$ be zero valued everywhere. In terms of correction of the wavefront (independent of any object information) we define the effective or resultant phase of aperture $j\in\mathcal{A}$ as the difference between incident wavefront phase $\tilde{\varphi}_j$ and the estimate used for inverse correction $\hat{\varphi}_j$,

$$\varphi_j=\tilde{\varphi}_j-\hat{\varphi}_j. \tag{9}$$

To achieve $\angle R_L=0$ means the correcting phases $\hat{\varphi}=[\hat{\varphi}_1\ \hat{\varphi}_2\ldots\hat{\varphi}_N]^T$ must all exactly match the corresponding unknown wavefront piston values. Instead, we can require that the autocorrelation phase $\angle R_L$ describe a tilt plane Ψ through the origin: other than applying a shift in the image position this would not cause any changes in I in the case of a filled aperture [8].

In terms of piston-only phase components in a dilute aperture, the effective phase patches in $\angle R_L$ must all be such that Ψ intersects their centers, describing a bisecting line across each as shown in Fig. 2. However, this means only those points within the phase patch that lie on this line will be properly phased—the areas on either side will retain some residual aberration, distorting the image slightly. To accomplish this piston phasing we must ensure that the effective aperture phase differences lie on Ψ. At the center of the $\angle R_L$ patch corresponding to the jth and kth aperture pair, the value of this piston-defined plane is denoted ψ_{jk}, i.e.,

$$\varphi_k-\varphi_j=\psi_{jk}. \tag{10}$$

By decomposing the effective phases as in Eq. (9) a system of equations can be constructed from Eq. (10) in terms of correcting phases $\hat{\varphi}_j$, $\angle R_L$ tilt plane phase ψ_{jk}, and wavefront aperture phases $\tilde{\varphi}$ for each of the $N(N-1)/2$ aperture pairs:

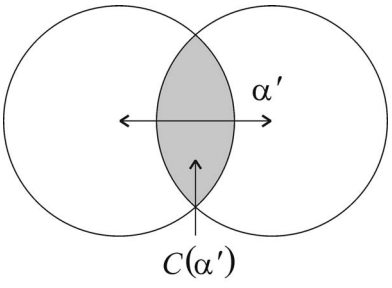

Fig. 1. Showing the overlapping region $C(\alpha')$ of two aperture functions relatively shifted by α'. The area of this region is $M_{jk}(\alpha')$ in Eq. (8).

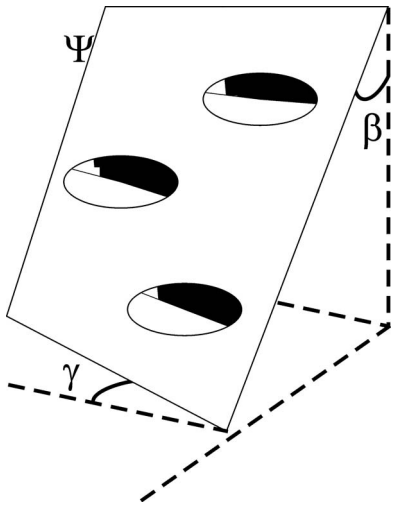

Fig. 2. Perspective diagram of a tilt plane bisecting the centers of $\angle R_L$ piston phase patches—the lighter side of the patch is before/above the tilt plane (partially transparent in the illustration), while the darker half is behind/below it. The angles β and γ indicate the two dimensions of tilt, with respect to the horizontal and vertical reference axes.

$$-\hat{\varphi}_k+\hat{\varphi}_j=\psi_{jk}-\tilde{\varphi}_k+\tilde{\varphi}_j. \tag{11}$$

The tilt plane defining the phase ψ_{jk} is unfixed since the autocorrelation phases depend on differences, and so far there is no prescribed reference level. Appending a condition fixing a single correcting phase to an arbitrary constant compels all others to be relative to it. Without loss of generality we make this constant zero, so we have

$$\begin{bmatrix}
1 & -1 & 0 & \cdots & & & 0\\
1 & 0 & -1 & 0 & & & 0\\
\vdots & & & \ddots & & & \\
1 & 0 & \cdots & & & & -1\\
0 & 1 & -1 & 0 & \cdots & & 0\\
\vdots & \vdots & & \ddots & & & \\
 & 1 & 0 & \cdots & & & -1\\
 & 0 & 1 & -1 & 0 & \cdots & 0\\
 & & 0 & \ddots & \ddots & & \\
 & & & & & & \\
0 & \cdots & & & & 1 & -1\\
1 & 0 & \cdots & & & & 0
\end{bmatrix}
\begin{bmatrix}\hat{\varphi}_1\\ \hat{\varphi}_2\\ \vdots\\ \hat{\varphi}_N\end{bmatrix}$$

$$=\begin{bmatrix}
\psi_{1,2}-\tilde{\varphi}_2+\tilde{\varphi}_1\\
\psi_{1,3}-\tilde{\varphi}_3+\tilde{\varphi}_1\\
\vdots\\
\\
\psi_{N-1,N}-\tilde{\varphi}_N+\tilde{\varphi}_{N-1}\\
0
\end{bmatrix}. \tag{12}$$

The system of Eqs. (12) relates the correcting phases $\hat{\varphi}$ to the tilt plane values ψ_{jk} and unknown aperture phases, subject to modulo 2π ambiguity. With more unknowns than knowns a calculable solution for the $\hat{\varphi}$ is yet un-

achievable. However, the properties—in both the matrix formulation and the autocorrelation—of redundant spacings [where two or more spacings are identical, i.e., $s_{jk}=s_{lm}$ is true, given some $(j,k),(l,m)\in\mathcal{A}^2$] form the basis of a calibration method. We show next that if sufficient redundancy exists, the whole system can be solved indirectly by making use of the autocorrelation magnitude as an evaluation function.

With reference to Eqs. (12), if a redundant spacing exists in the array, the autocorrelation tilt phase for both aperture pairs must be identical, i.e., $\psi_{jk}=\psi_{lm}$, thus making it possible when carrying out row reduction to replace an equation with a redundant condition

$$\hat{\varphi}_k-\hat{\varphi}_j-\hat{\varphi}_m+\hat{\varphi}_l=\tilde{\varphi}_k-\tilde{\varphi}_j-\tilde{\varphi}_m+\tilde{\varphi}_l. \tag{13}$$

The greatest number of such independent redundant conditions possible is $N-3$ [6]. In this case the matrix can be reduced to N-square, with $N-3$ rows in the form of Eq. (13), the single reference-level correcting phase, and two rows with constant terms involving a ψ_{jk} with $j,k=1,2,\ldots,N$.

The system of Eqs. (12) was constructed on the premise that the effective phase differences were all centered on the $\angle R_L$ tilt plane Ψ. Thus, the value of these two ψ_{jk} [dependent on the differences $-\hat{\varphi}_k+\hat{\varphi}_j$ as in Eq. (11)] completely specifies Ψ, provided the spacings corresponding to the chosen pairs of apertures are not antiparallel.

The importance of redundant spacings on the autocorrelation can be seen from Eq. (14) below. Noting the constraint that the apertures be small enough and the array configuration such that there is no overlapping of nonzero cross correlation magnitude regions in R_L, the autocorrelation in the contiguous region around $\alpha=s_{jk}=s_{lm}=\ldots$ corresponding to redundant spacings will be the sum of complex values over only those aperture pairs $(j,k),(l,m)\in\mathcal{A}^2$:

$$\begin{aligned}R_L(\alpha)&=\sum M_{jk}(\alpha-s_{jk})\exp[i(\varphi_k-\varphi_j)]\\&=M_{jk}(\alpha-s_{jk})\exp[i(\varphi_k-\varphi_j)]\\&\quad+M_{lm}(\alpha-s_{lm})\exp[i(\varphi_m-\varphi_l)]+\cdots\\&=M_{jk}(\alpha-s_{jk})\{\exp[i(\varphi_k-\varphi_j)]\\&\quad+\exp[i(\varphi_m-\varphi_l)]+\cdots\},\end{aligned} \tag{14}$$

with the last equality because $M_{jk}=M_{lm}=\cdots$.

Considering just a pair of redundant spacings, it can be shown that the modulation transfer function $|R_L(\alpha)|$ is proportional to the cosine of the phase difference, i.e.,

$$|R_L(\alpha)|=2M_{jk}(\alpha-s_{jk})\cos\left(\frac{\varphi_k-\varphi_j}{2}-\frac{\varphi_m-\varphi_l}{2}\right). \tag{15}$$

Thus, the magnitude will be maximized if and only if both components have identical effective phase difference, i.e., $\varphi_k-\varphi_j-\varphi_m+\varphi_l=0$. This is the same as the redundant condition (13) satisfying the system of equations relating to the tilt plane Ψ. Furthermore, it may be true that the array configuration generates identical redundant condition equations, as in condition (13), at a number of different redundant spacings, for example, in a parallelogram configuration $s_{jk}=s_{lm}$ and $s_{jl}=s_{km}$, with $s_{jk}\neq s_{jl}$. In this case, all but one of the four conditions relating to this parallelogram is eliminated from Eqs. (12) by simple row operations, while $|R_L(\alpha)|$ at frequencies formed from the same aperture combinations $\alpha=s_{jk},s_{jl}$ behaves identically under changes in $\hat{\varphi}$, as can be seen from Eq. (15).

If the autocorrelation at a given α is from a single spacing s_{jk} only, $|R_L(\alpha)|$ will be given, from Eq. (8), by the single R_{jk} magnitude component

$$|R_L(\alpha)|=M_{jk}(\alpha-s_{jk}), \tag{16}$$

which is independent of phase and so constant regardless of the $\hat{\varphi}$. Hence, the integral of $|R_L|$ is insensitive to any effective phase difference between apertures not involved in redundant spacings. This integral therefore serves as an evaluation function for $\hat{\varphi}$, being maximized if and only if $\hat{\varphi}$ satisfies the matrix Eq. (12), and is immune to the fact that the $\tilde{\varphi}_j$ are unknown in the system. This means all the $\angle R_L$ patches lie on the tilt plane Ψ. Note, however, that the above description ignores the modulo 2π characteristic of phase measurements. That modulo arithmetic can lead to a finite set of ambiguous solutions has been noted [6] and will be considered in more detail in subsequent sections.

As described in Eq. (8) an image is sharpened by maximization of the integral of the intensity squared. Referring to Eq. (1), it is seen that I and the product R_LU are a Fourier transform pair. Consequently, by Parseval's theorem

$$\frac{1}{2\pi}\int|I(\xi)|^2d\xi=\int|R_L(\alpha)|^2|U(\alpha)|^2d\alpha, \tag{17}$$

implying that, because $|U|$ is fixed, changes only in $|R_L|$ will be reflected in the image sharpness integral on the left. Furthermore, because $|U|$ is positive definite, maximization of $|R_L|$ corresponds with maximization of the $|I|^2$ integral: the image sharpness will be maximized when the autocorrelation magnitude is maximized. This can be used to determine when the redundant spacing conditions are satisfied, yielding wavefront aperture phases corrected to produce a piston-defined tilt plane in $\angle R_L$ and a pseudo-diffraction-limited image of the object.

Figure 3(b) shows the unaberrated PSF, with maximum sharpness, from the 12-aperture array in Fig. 3(a). There the central peak possesses the majority of the energy, with low surrounding grating responses producing faint (but not insignificant) alias images. With an arbitrary piston-defined tilt plane Fig. 3(c) shows a PSF with grating structure shifted relative to the fixed envelope function such that a number of peaks and corresponding alias images are approximately evenly weighted, but still with maximum sharpness. From a phenomenological viewpoint, the fringe systems that compose the image reconstruction maintain their relative positioning, and hence areas of overlap of the PSF envelope function are also the same. Under an applied piston-defined tilt phase, energy in each fringe set is shifted in the direction of the tilt, and that which disappears from one side of the PSF re-enters at the other since the structure is repeated *ad infinitum*. The energy distribution within the overlap areas is maintained and hence so is the sum of the squares (or higher powers). However, because of the changed PSF

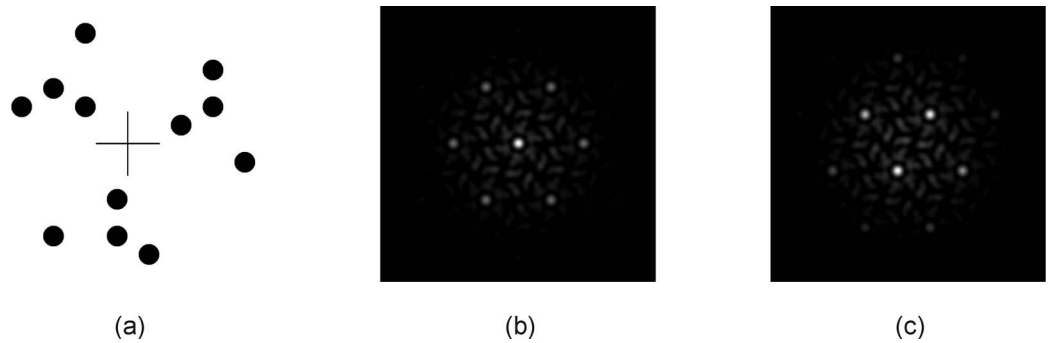

Fig. 3. Showing in (a) a 12-element dilute aperture (center marked with a cross), (b) its unaberrated PSF, and (c) the PSF subject to a piston-defined tilt plane.

the resulting image is not identical to an unaberrated image.

In Fig. 4 the effect of the piston-defined tilt plane is illustrated by imaging the circular object in 4(a) with the 12-aperture array of Fig. 3(a), scaled to produce a PSF large relative to the image. The image without any tilt is seen in Fig. 4(b) and with piston-defined tilt in 4(c). Replication of the circle is seen, with positioning and weighting corresponding to the grating response peaks in the PSFs of Figs. 3(b) and 3(c). Contrast is reduced and distortion introduced in Fig. 4(c) compared to 4(b) due to the aliases being afforded even weighting, making it much harder to distinguish them, yet there is no difference in image sharpness.

In the second row of Fig. 4(a) familiar object 4(d) is shown imaged in the absence of aberration by the same 12-aperture array with the same scaling 4(e) and with the same piston-defined tilt in 4(f) as above. The replication of

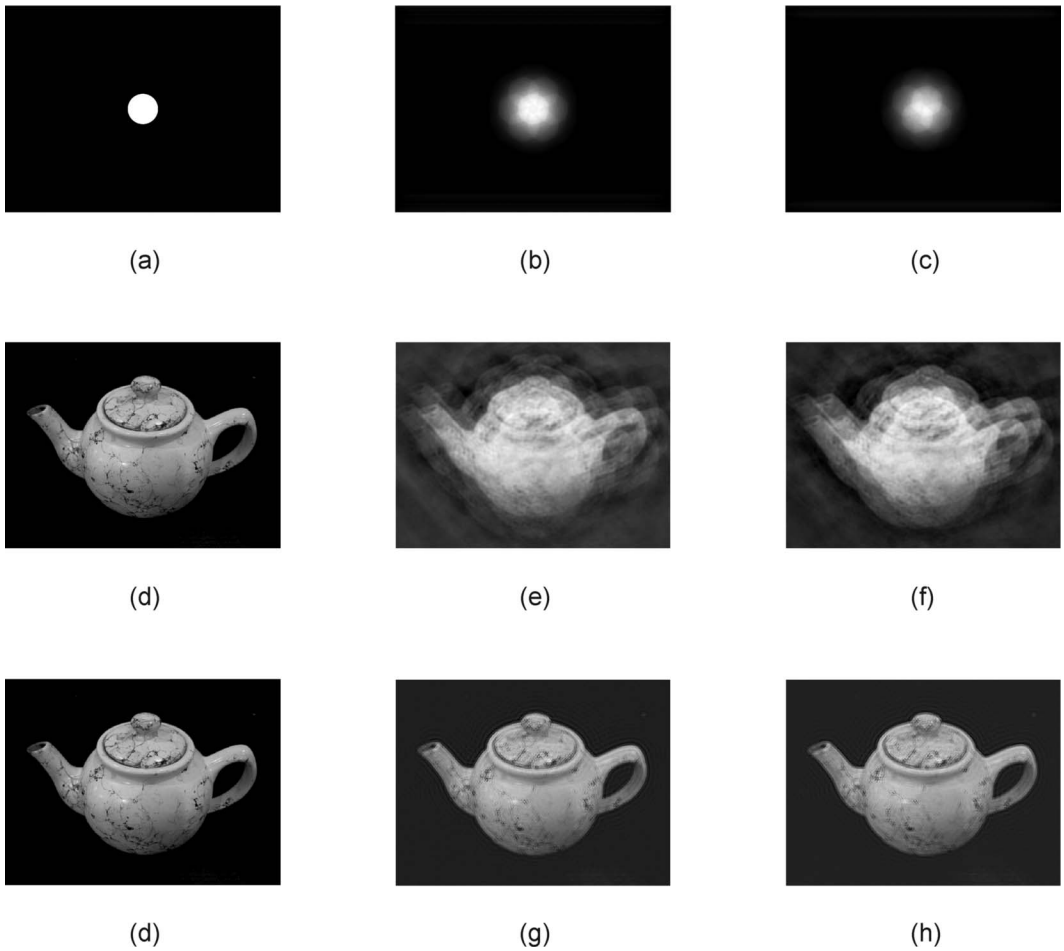

Fig. 4. Showing on the first row: (a) a simple circular source, (b) the unaberrated image of (a) produced by the 12-aperture array of Fig. 3(a), and (c) the image resulting from the PSF of Fig. 3(c). The second row shows an object which is (d) imaged by the same 12-aperture array producing a large PSF to illustrate the image aliasing, unaberrated (e), and with the same PSF as in (c) to give (f). The third row shows the object repeated in (d) for convenience, (g) imaged unaberrated using again the same array with a higher resolution PSF, and (h) with the same piston-defined tilt plane PSF.

structure can be identified in both 4(e) and 4(f), and the relative differences between them seen to correspond again with the PSFs in Figs. 3(b) and 3(c). Reduced contrast between aliases in 4(f) compared with 4(e) is also seen. When the size of the PSF relative to the image is realistically small, as is shown in Figs. 4(g) and 4(h), the alias images are much closer together. Although these images appear similar, reduced contrast between aliases in the piston-defined tilt image is always present, as described above, regardless of the particular piston-defined tilt plane. The unaberrated case will therefore always be marginally superior, independent of the imaging resolution. Again however, image sharpness is maximized in both cases.

Although image sharpness is insensitive to the relative positioning of the PSF envelope and underlying grating structure because of the piston-defined tilt plane, there remains the possibility that another evaluation metric may be used to identify the compensatory aperture-tilt shift necessary to colocate the two. Since contrast between image aliases is affected by the tilt plane, this may form the basis of such a metric. It is difficult to envisage at this stage how this might be accomplished without prior knowledge of the object, however.

D. Phase Retrieval RSC

Although an approach to phase retrieval has previously been reported [6], we are presenting phase retrieval in this slightly different form directly applicable to wavefront sensing in order to draw analogies with the theory of the image sharpness method and so that the issues of solution ambiguity might be discussed in common terms.

In Eq. (1), we represent incoherent image formation in terms of the modulation of the object brightness distribution's Fourier transform U by the autocorrelation R_L of the aperture-sampled wavefront. In Subsection 2.C we have described an approach for correcting the wavefront aperture piston phases—made possible only by the presence of redundancy in the array spacings—that relied on the maximization of the autocorrelation magnitude $|R_L|$. As an alternative to this direct correction, treating the wavefront aberration at each aperture as piston-only, we can calculate information about the aperture phases explicitly. A system of linear equations can be constructed involving the aperture aberration and object phases by making use of their relationships as expressed in $\angle[R_L U]$ from Eq. (1). In the same way as the image sharpness method, the solution relies on the presence of sufficient redundancy, but this time its interpretation is in terms of object information.

Considering a single point at the center of each autocorrelation patch corresponding to $R_L(\alpha)$ at $\alpha = s_{jk}$ given any $(j,k) \in \mathcal{A}$, it can be seen from Eq. (8) that the phase relationship of a nonredundant spacing can be written as

$$\angle[R_L(\alpha)U(\alpha)] = \angle[R_{jk}(\alpha - s_{jk})U(\alpha)] = \tilde{\varphi}_k - \tilde{\varphi}_j + \theta_{jk}, \tag{18}$$

where θ_{jk} is the object phase component sampled by spacing s_{jk}, and $\tilde{\varphi}_j$ and $\tilde{\varphi}_k$ are the wavefront aperture phases (using the same notation as earlier for consistency).

Now, from Eq. (1), taking the Fourier transform of the image I and denoting the measured phase component at spatial frequency s_{jk} as μ_{jk}, a system of $N(N-1)/2$ independent equations can be formed as

$$\tilde{\varphi}_k - \tilde{\varphi}_j + \theta_{jk} = \mu_{jk}. \tag{19}$$

If the aperture phases were correctly known, the object phases could be solved from this in terms of the measurements μ_{jk}. When dealing with redundant spacings, $R_L(\alpha)$ is the sum of a number of cross correlations as shown in Eq. (14), so Eq. (18) is not applicable. If only a pair of redundancies is present at α, however, a simple experimental method can be used to measure separately the two Fourier phases [9]; μ_{jk} for each $(j,k) \in \mathcal{A}$ is then available, so Eq. (19) can be formed for all $N(N-1)/2$ spacings. However, the rank of the system is deficient by N, corresponding to the unknown aperture phases $\tilde{\varphi}_j$, which are to be found. As with image sharpness correction, the presence of redundancies in the array allows this to be accomplished.

Rearranging Eq. (19) so that the object phase appears on the right-hand side allows a system of equations with the form of

$$\tilde{\varphi}_k - \tilde{\varphi}_j = \mu_{jk} - \theta_{jk} \tag{20}$$

to be constructed. As was the case for equations formed from relation (11), this system involves only differences, so to be nonsingular requires a fixed reference level to be defined by appending an equation that sets one $\tilde{\varphi}_j$ to zero. The result relates the $\tilde{\varphi}_j$ to the unknown θ, but as before a calculable solution is as yet unachievable. However, sampled object information is identical from vector spacings that are the same. This implies that any discrepancy between the measured phases of identical spacings is due entirely to the aperture phases. If the aperture array possesses $N-3$ independent redundant conditions, this many equations in the row-reduced system can therefore be written in the form

$$\tilde{\varphi}_k - \tilde{\varphi}_j - \tilde{\varphi}_m + \tilde{\varphi}_l = \mu_{jk} - \mu_{lm}, \tag{21}$$

leaving two in the form of Eq. (20). To eliminate the unknowns from these, we may take advantage of the addition of a tilt plane resulting merely in an arbitrary shift in the image.

If we hypothesize the addition of a tilt plane to $\angle R_L$, an identical function with opposite gradient is implied in the object information $\angle U$ by the observed data. Denoting as ψ_{jk} the phase added to $\angle R_L(\alpha)$ at each point $\alpha = s_{jk}$ (and correspondingly subtracted from the θ_{jk}), the autocorrelation and object phases at these α are written as $\tilde{\varphi}'_k - \tilde{\varphi}'_j = \tilde{\varphi}_k - \tilde{\varphi}_j + \psi_{jk}$ and $\theta'_{jk} = \theta_{jk} - \psi_{jk}$, respectively. This change does not alter the redundant conditions of Eq. (21), as the ψ_{jk} cancel, allowing them to be written as

$$\tilde{\varphi}'_k - \tilde{\varphi}'_j - \tilde{\varphi}'_m + \tilde{\varphi}'_l = \mu_{jk} - \mu_{lm}, \tag{22}$$

putting the tilted aperture phases in terms of measured data only. The two nonredundant equations now have the form $\tilde{\varphi}_k - \tilde{\varphi}_j + \psi_{jk} = \mu_{jk} - \theta_{jk} + \psi_{jk}$; the tilt plane in $\angle R_L$ is then fixed by specifying the tilted object phase at the two $\alpha = s_{jk}$ be equal to known constants, $\psi_{jk} - \theta_{jk} = const$, where again zero is used for simplicity. This implies that the

$\angle R_L(\alpha)$ at these points will be equal to the measured phase values, i.e., $\tilde{\varphi}'_k - \tilde{\varphi}'_j = \mu_{jk}$. The wavefront piston phases $\tilde{\varphi}'_j$, which are subject to the tilt plane applied in $\angle R_L$, can then be solved.

Written in terms of these variables, the system of equations concomitant with Eq. (19) have the form

$$\tilde{\varphi}'_k - \tilde{\varphi}'_j + \theta'_{jk} = \mu_{jk}. \tag{23}$$

From this we can now find the tilted object phases θ'_{jk} if required.

3. SOLUTION AMBIGUITY

A. Modulo 2π Arithmetic in Linear Algebra

We have seen that solving for aperture phases, whether in terms of indirect correction or direct calculation, is based on essentially the same linear system with the form $Ax = y$. Usually the variables and constants in such systems are real numbers. When dealing with phases, however, the origin is a branch point and phases are modulo 2π. By looking at the properties of such a system with integer matrix coefficients as in RSC, the presence of and conditions for ambiguous solutions to the RSC problem can be seen [6].

From the relation $Ax = y$, if A is full rank and n square it can be formed into an upper triangular matrix A' by Gaussian elimination. Denoting as y' the vector of constants changed by the same row operations, backward substitution yields the elements of x in the form

$$x_j = \frac{y'_j - \Sigma_{m=j+1}^{n} a'_{jm} x_m}{a'_{jj}}, \tag{24}$$

where integer a'_{jj} is the jth coefficient on the leading diagonal of A'. The numerator consists of sums of elements that are modulo 2π, and so the result is also modulo 2π. Therefore if and only if a'_{jj} has unit magnitude will there be no uncertainty about the Riemann sheet of x_j, and the x_j be unambiguous. As noted earlier, if the y_j are real numbers the summations do not cross branch lines and the Riemann surface consists of only a single sheet; the solutions are, therefore, unique and free of ambiguity.

Similarly as noted in [6], the essential property of these matrices, revealing the presence of ambiguity, is the determinant. Ambiguity in the solution arises if and only if the determinant of A has nonunit magnitude.

In RSC, the constants are exclusively phases. In the image sharpness formulation, the elements of y are either identically zero, corresponding to *a priori* conditions, or combinations of wavefront aperture phases for redundant conditions, as shown in the right-hand side of Eq. (13). Similarly, with phase retrieval the nonzero constants in the aperture phase subsystem are sums of a number of measured phases μ_{jk}. Therefore in both cases the constants are modulo 2π, and the preceding analysis is applicable to RSC systems. Instead of being unique, solutions of RSC linear systems, regardless of the evaluation metric used, may therefore be ambiguous unless such care is taken in the array design that it leads to a matrix with unit determinant.

B. RSC Imaging with Ambiguities

The impacts of the ambiguity on image quality in the image sharpness and phase retrieval methodologies are closely related, even though the methods of finding the solutions are quite different. The linear system in image sharpness originates directly from the equations placing all autocorrelation phase patches on the predefined tilt plane. The presence of sufficient redundancy allows this to be achieved without possessing information on the required phase of each patch in $\angle R_L$ and true wavefront aperture phases $\tilde{\varphi}$, both of which are unknown *a priori*. We have shown that the integral of the auto-correlation magnitude plane is maximized if and only if the redundant conditions are satisfied, i.e., at a solution of the linear system describing correction of the wavefront aperture phases. However, this equivalence means ambiguity can be present in the image sharpness criterion also; that is, when the redundant and *a priori* conditions are such that the linear system cannot be solved uniquely, it is possible for the sharpness criterion to be maximized but to produce an aberrated image. The correction phases in $\hat{\varphi}$ may be erroneous, causing the patches in $\angle R_L$ not to sit on the tilt plane and the sampled object phases in U to be aberrated. The $\angle R_L$ patches, and thus the U phases, will be found in any one of a discrete set of locations dependent on the determinant magnitude: if $|\det A| = 2$, two such values will exist (one correct, one incorrect); if $|\det A| = 3$ there will be three such sites (but always only one correct), and so on.

Turning to phase retrieval, if errors are present in the subsystem of aperture phases, they will be propagated into the object phases as the data inversion proceeds. Under identical aberration, the errors in the object phase will exactly match those resulting from the erroneous image sharpness correction. Consequently, the reconstructed object will have the same distortion as the image from active correction.

C. *A priori* Conditions and Array Design

In both image sharpness and phase retrieval approaches to RSC, the determinant of the system of phase relations has been shown to indicate the possible introduction of solution ambiguity. To illustrate conditions that may result in this ambiguity, Figs. 5(a) and 5(b) show two aperture arrays with superficially similar properties—both have the same number of apertures and both sample a similar set of spatial frequencies because of their similar geometry. Figure 5(a) contains only redundancies in linear arrangement, i.e., redundant spacings that involve three apertures in a line, whereas Fig. 5(b) contains many four-aperture redundancies in parallelogram layout. The type of redundancy is further illustrated below each array picture: three apertures in a line giving one redundancy condition in which the central aperture is involved twice [Fig. 5(c)], and four apertures in a line considered as the limits of a parallelogram where the angles between the sides are zero and π radians [Fig. 5(d)]. Such a parallelogram (collapsed or not) provides two redundancy conditions, each aperture involved only once in each redundancy.

The linear arrangement where one of the apertures is involved twice in a redundancy means a reduction in the independence of parameters, leading to ambiguity in

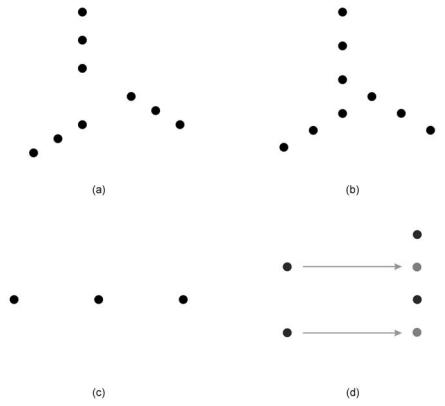

Fig. 5. Showing two nine-aperture redundant spacing arrays with similar but subtly different configurations. The redundancies in (a) are made solely from three-aperture linear arrangements as in (c), whereas in (b) there are many parallelogram redundancies, collapsed as shown in (d) such that sides of the parallelogram formed by black dots all become parallel as one set of dots is shifted to lie co-linear with the others (becoming gray).

identifying the phase of piston aberration components. This can be seen in the following simple phase retrieval calculations for a three-aperture and a four-aperture array.

Referring to the established form for the phase relations of the array in Eq. (20), measurement phases between numbered aperture pairs are equal to object phases plus instrument aberration phase terms. Account is explicitly taken here of the modulo 2π nature of the arithmetic for a limited selection of equations that highlight the process:

$$\mu_{12} = \theta_{12} + \varphi_1 - \varphi_2 \pm 2n_{12}\pi,$$

$$\mu_{13} = \theta_{13} + \varphi_1 - \varphi_3 \pm 2n_{13}\pi,$$

$$\mu_{23} = \theta_{23} + \varphi_2 - \varphi_3 \pm 2n_{23}\pi,$$

$$\mu_{34} = \theta_{34} + \varphi_3 - \varphi_4 \pm 2n_{34}\pi, \tag{25}$$

where n_{jk} is an integer.

Three-aperture redundancy case [first three relations in system (25) refer to this case]. Taking the redundant condition, $\theta_{12}=\theta_{23}$ and rearranging in terms of measurements gives $(\mu_{12}-\mu_{23})\pm 2n_r\pi=\varphi_3-2\varphi_2+\varphi_1$. Substituting into this from the second equation of system (25) gives $\mu_{12}-\mu_{23}+\mu_{13}\pm 2n\pi=\theta_{13}+2\varphi_1-2\varphi_2$. Finally, setting the disposable parameters $\theta_{13}=0$ and $\varphi_1=0$, we get

$$M/2 \pm n\pi = -\varphi_2, \tag{26}$$

where $M=\mu_{12}-\mu_{23}+\mu_{13}$ is the measurement phase resultant. Thus φ_2 is subject to an $n\pi$ ambiguity, giving two possible solutions—one for n even and one for n odd.

Four-aperture case [here all relations in system (25) are applicable]. Again setting the redundant condition, this time $\theta_{12}=\theta_{34}$, and rearranging in terms of measurements we get $(\mu_{12}-\mu_{34})\pm 2n_r\pi=\varphi_1-\varphi_2-\varphi_3+\varphi_4$. This condition is one of two identical redundancy conditions that may be obtained from consideration of the phases corresponding to parallel sides of a parallelogram. Because the condition involves all four collectors, there is no coefficient 2 in the equation (cf. the three-aperture case discussed above). These statements remain true even if the parallelogram is collapsed to a line. The uncertainty on the measurement phase will not be divided by 2 and will remain modulo 2π.

The factor of 2 that appears in the case of linear redundancies is equivalent to introduction of a value with magnitude of 2 on the leading diagonal of the triangular matrix form, that if left uncanceled produces a nonunit determinant. To illustrate this development of nonunit-magnitude determinant from linear redundancy entries in the matrix, we formulate the RSC matrix in Fig. 6, involving one such redundancy in the penultimate row. For completeness we have returned to the full formulation of the matrix used for object phase retrieval [6]. Row reduction is performed to present the redundancy information in triangular form in the lower right-hand matrix partition (labeled block D), which may be recognized as the form of the aperture phase system described in subsection 2.D.

In Fig. 6 the row reduction process is highlighted for this linearly redundant relation as it progresses through the matrix. The arrows show which object phases in the object parameter selection block A are involved in this redundancy. The highlighted rows show which aperture piston phases in selection block B correspond to these. The encircled elements within the same column demonstrate that the same aperture is involved twice, here producing a factor of 2 in block D when these rows are subtracted. Possibilities to cancel these 2's exist when reducing to triangular form, namely by elimination with other redundancies involving the same aperture or with disposable parameters. As the ratio of linear redundancies to parallelograms increases the possibilities for achieving this diminish.

D. Additional Considerations

The preceding section applies to the phase retrieval case where phase measurements are made, but it can be seen

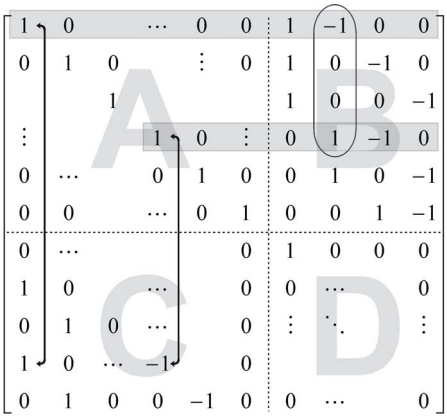

Fig. 6. (Color online) Progression of linear redundancy information by Gaussian elimination, resulting in factors of 2 in the triangular form of block D. The figure illustrates a redundancy condition (in block C) that can be used in combination with measured phase data (rows through blocks A and B) to produce an upper-triangular matrix. Addition and subtraction of the rows from A, B set the correspoding elements in C to zero, but lead to a matrix element with value 2 in block D due to the elements identified by the lozenge in block B.

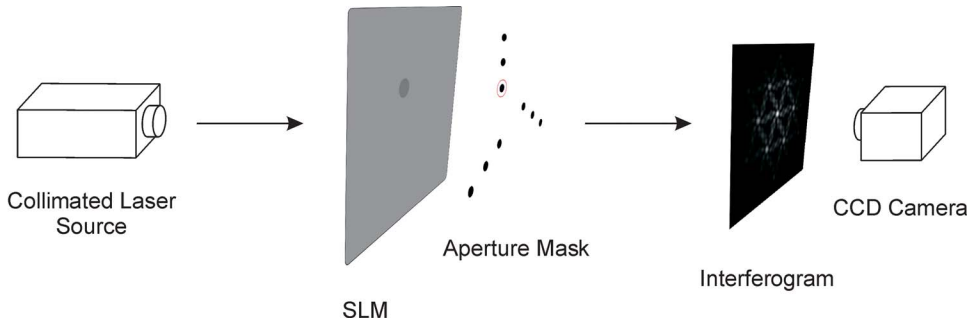

Fig. 7. (Color online) Experimental setup of the laboratory demonstration of visibility on linearly redundant baselines. A collimated laser source is projected onto a liquid crystal SLM which is programmed to modulate the phase of a disk corresponding to the selected inner aperture of the RSC mask (indicated). This light then passes through the aperture array and the resulting interferogram is imaged on a CCD camera.

also to apply to the image sharpness case as the following experiment demonstrates.

The nine-aperture array shown in Fig. 3(a) was manufactured (by hand measurement and drilling of a steel mask) and illuminated by collimated laser light. One of the inner three apertures was modulated in phase from 0 to 1 wave of error using an optically addressed spatial light modulator (SLM), and the resulting interferogram imaged on a CCD camera, as shown in Fig. 7. The data pertaining to individual frequency components were then extracted by Fourier transform, and the visibilities are plotted in Fig. 8. Visibilities change according to relation (15), but where the aperture is central in a linear redundancy we have $j=m$ and as shown in Eq. (26) this results in an $n\pi$ phase ambiguity, i.e., visibility can remain maximized when frequency content sampled by linear redundancies is out of phase by $n\pi$. This is manifested in the plot as the visibility changing twice as quickly for baselines where the aperture is central as compared with the curve corresponding to a redundancy that involves the aperture situated at the end.

Determinants are used to calculate volumes in vector calculus: the absolute value of the determinant of real vectors is equal to the volume of the n-dimensional parallelepiped spanned by those vectors [10]. The more orthogonal the row vectors in the matrix are, the larger this volume will be and hence the larger the determinant. Conversely, the more orthogonal the row vectors, the lower the condition number, and so the matrix determinant is inversely correlated with the condition number. Methods exist in numerical analysis for improving conditioning [11] so more emphasis should be placed on obtaining low determinant.

To conclude, it is better to limit the presence of linear-type redundancies for the purpose of extracting phase uniquely. The array design always permits great flexibility on the spatial frequency coverage attained, and this restriction does not impinge significantly on the image quality that can be achieved.

4. DISCUSSION

Throughout, we have maintained the condition that the illumination amplitude falling on every aperture is constant across the array. This allows us to describe explicitly the characteristics of the image sharpness criterion under aberration and correction of piston phases and improves the error properties of the phase retrieval method. If this condition is relaxed, such that the illumination across each aperture remains constant but is different from one aperture to another, both of these advantages are lost. In the image sharpness case, the magnitude components of the terms in Eq. (8) will be different. Figure 9(b) illustrates that when this is the case, the variability of redundant peaks is diminished as compared with when the magnitude components are the same [Fig. 9(a)]. Consequently, the sensitivity of the redundant peaks to changes in the correcting phases will be reduced. If this were to happen, it would follow that the accuracy of the correcting phase estimator would be compromised.

Similarly, differing illumination conditions across the apertures in the phase retrieval method will cause

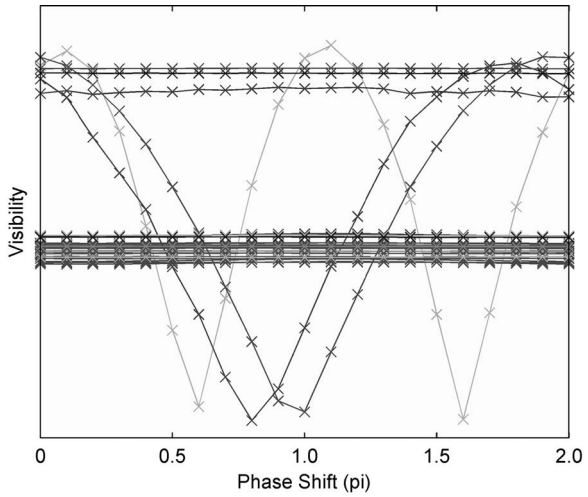

Fig. 8. Laboratory demonstration of visibility on linearly redundant baselines. The array configuration is that of Fig. 5(a), and one of the three innermost apertures is the one modulated. This is central (and hence involved twice in the redundancy equations) in a single pair of linearly redundant spacings, so the visibility changes at twice the rate of the two other linearly redundant baselines, where it is situated at the end. Visibilities from nonredundant baselines remain constant (within experimental error) and clustered around the center of the plot, while those due to redundant baselines whose phase is not being modulated are constant and clustered toward the top. The displacement seen between the single cycling visibilities is due to additional aberrations in the optical setup, and the spread of visibilities is because of nonuniformity in the light source.

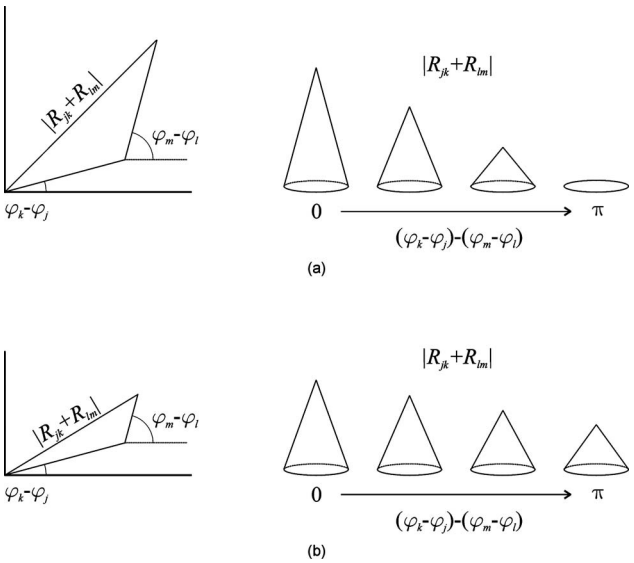

Fig. 9. Combination of complex cross correlation components for redundant spacings $s_{jk}=s_{lm}$ and $s_{jl}=s_{km}$ with $s_{jk}\neq s_{jl}$. Where the illumination is the same on all apertures (a), the autocorrelation magnitude peaks will vary according to Eq. (15) between the maximum when the phasors are parallel and zero when they are antiparallel. If the illumination is different (but constant across any particular aperture) (b), the relative maximum peak height will be reduced as compared with (a), and the minimum will be greater.

greater uncertainty in the Fourier transform phase measurements, leading to poorer accuracy of the aperture and object phase calculations. Though this paper treats the solution to the imaginary part of the log complex amplitude, it may be possible by use of greater levels of redundancy to calibrate for the illumination level also. Such increased levels of redundancy, however, may increase the system determinant and thereby compromise the integrity of the phase solution.

Throughout the analysis we have made no consideration of anisoplanatism, the implication being that all scenes are observed isoplanatically. Of course, in astronomical imaging this premise may not be true, and consequently, the image observed may not correspond exactly with that modeled. Furthermore, precise location and sizing of the apertures involved in redundant spacings has been assumed in the theory. Mislocation of the apertures involved in redundant spacings will corrupt the autocorrelation phase at the repeated spacings because, although the piston phase differences in Eqs. (14) will be unchanged within the remaining shared frequency content, the magnitude components will no longer be as they ideally would, so the complex sum has different resultant argument. This is a source of error similar to that described above when the illumination over redundant spacings is not constant. Also, the phase calculation in the Fourier transform of frequency components with reduced magnitude will be intrinsically less accurate, introducing a further source of random error.

This result of mislocated apertures in the autocorrelation being akin to nonconstant illumination means that image sharpness calibration is affected in the same way as described earlier; namely, in the autocorrelation patch, where aperture pair cross correlations overlap, the magnitude peak heights will be less sensitive to changes in aperture phase, so making the sharpness optimization less accurate. However, when the mislocations are small the errors are relatively minor also, because the area of overlap of circular aperture pairs is less sensitive to such mislocations than to larger ones. As noted earlier, experience indicates that the vector spacings should be accurate to about 10% of the aperture diameters. The presence of apertures with different radii in the array also introduces uncertainty into the magnitude components of cross correlation terms in Eqs. (14), so again the complex sum has a phase different from the correct value and a smaller magnitude that is less sensitive to changes in phase difference of the contributing aperture pairs. Robustness to minor shape, size, and positioning errors is evidenced by the experimental demonstration of image sharpness RSC shown in Fig. 8, which used a hand marked and drilled aperture mask.

5. CONCLUSIONS

We have shown methods for calculating unknown aperture piston phase parameters subject to a uniform tilt, and for performing active correction of piston phases in the synthetic imaging problem, important in all optical interferometry applications such as astronomical, space, and ground based observation and high-resolution military surveillance from mobile platforms. In this methodology dilute arrays are designed with redundant spacings, providing repeated measurements to allow detection of aberrations. The phase calculation approach can be used as a method for synthesizing a reconstruction of the object brightness distribution subject to an arbitrary shift, or as a wavefront sensor. Correction utilizing image sharpness as an evaluation function results in a pseudo-diffraction-limited synthetic image of the object. We have shown that in using this indirect calibration method an increase in image aliasing and corresponding loss of contrast will be observed.

In addition to aliasing and incomplete frequency coverage, image fidelity is also affected by solution ambiguity and it has been shown that in order for an unambiguous solution to be achieved, the system of phase relations needs to possess unit determinant. We have demonstrated that for this purpose the presence of linear-type redundancies in the array needs to be limited. The preference for the use of parallelograms (whether collapsed into a line or not) in array design reduces the array efficiency in providing Fourier space coverage since it implies the introduction of two redundancies rather than one redundancy for each collector in the array. However, use of parallelograms provides added protection against the selection of a low-modulus source Fourier component as a calibration point and mitigates against modulo-arithmetic-induced ambiguities by reducing the potential for the matrix to have nonunit determinant. We have shown that ambiguities resulting from modulo arithmetic are present in an image sharpness analysis as well as in direct inversion of RSC matrix algebra.

The effects of phase aberration with components other than piston alone is the subject of a future publication. Though the experimental result shows RSC is robust to

small errors in array geometry, a quantitative analysis of the impact of this and the remaining assumptions, namely anisoplanatic conditions and nonuniform illumination over the array, is an avenue for future research.

ACKNOWLEDGMENTS

The work presented here was carried out under the sponsorship of the Electro Magnetic Remote Sensing Defence Technology Centre (EMRS DTC), Particle Physics and Astronomy Research Council (PPARC), and the U.S. Air Force Office of Scientific Research (AFOSR), Air Force Materiel Command (AFMC), under grant FA8655-05-1-3050. The U.S. government is authorized to reproduce and distribute reprints for government purposes notwithstanding any copyright notation thereon.

The views and conclusions contained herein are those of the authors and should not be interpreted as necessarily representing the official policies or endorsements, either express or implied, of the U.S. Air Force Office of Scientific Research or the U.S. Government.

REFERENCES

1. R. K. Tyson, *Principles of Adaptive Optics* (Academic, 1991).
2. A. H. Greenaway, "Terrestrial Optical Aperture Synthesis Technique (TOAST)," Opt. Commun. **58**, 149–154 (1986).
3. J. T. Armstrong, D. Mozurkewich, L. J. Rickard, D. J. Hutter, J. A. Benson, P. F. Bowers, N. M. Elias II, C. A. Hummel, K. J. Johnston, D. F. Buscher, J. H. Clark III, L. Ha, L.-C. Ling, N. M. White, and R. S. Simon, "The Navy Prototype Optical Interferometer," Astrophys. J. **496**, 550–571 (1998).
4. M. J. Creech-Eakman, E. J. Bakker, D. F. Buscher, T. A. Coleman, C. A. Haniff, C. A. Jurgenson, D. A. Klinglesmith III, C. B. Parameswariah, V. D. Romero, A. V. Shtromberg, and J. S. Young, "Magdalena Ridge Observatory Interferometer: status update," Proc. SPIE **6268**, 62681V (2006).
5. A. M. Johnson, R. J. Eastwood, and A. H. Greenaway, "Optical aperture synthesis," in presented at the 3rd Electro Magnetic Remote Sensing Defence Technology Centre (EMRS DTC) Technical Conference, Edinburgh, Scotland, July 13–14, 2006. Available at http://www.emrsdtc.com/conferences/2006/confer_material.htm (last accessed December 15, 2008).
6. A. H. Greenaway, "Self-calibrating dilute-aperture optics, in digital image synthesis and inverse optics," Proc. SPIE **1351**, 738–748 (1990).
7. M. Born and E. Wolf, *Principles of Optics* (Pergamon, 1995).
8. R. A. Muller and A. Buffington, "Real-time correction of atmospherically degraded telescope images through image sharpening," J. Opt. Soc. Am. **67**, 1200–1210 (1974).
9. P. M. Blanchard, A. H. Greenaway, R. N. Anderton, R. Appleby, "Phase calibration of arrays at optical and millimeter wavelengths," J. Opt. Soc. Am. A **13**, 1593–1600 (1996).
10. J. H. Hubbard and B. B. Hubbard, *Vector Calculus, Linear Algebra, and Differential Forms: A Unified Approach* (Prentice-Hall, 2002).
11. R. Kress, *Numerical Analysis* (Springer, 1998).